Structural and Conformational Transformations in Self-Assembled Polypeptide−Surfactant Complexes

Sirkku Hanski, Susanna Junnila, László Almásy, Janne Ruokolainen, and Olli Ikkala*

Laboratory of Molecular Materials, Department of Engineering Physics and Mathematics and Center for New Materials, Helsinki University of Technology, P.O. Box 5100, FIN-02015 TKK, Espoo, Finland

Received August 29, 2007; Revised Manuscript Received November 13, 2007

ABSTRACT: Self-assembled polypeptide−surfactant complexes are usually infusible solids in the absence of solvent and do not allow fluidlike liquid crystallinity even when heated, which seriously limits their polymer-like applications in the solid state due to processing problems. This work is partly inspired by nature's liquid crystalline processing of silk and subsequent structural interlocking due to β-sheet formation. We demonstrate here polypeptide−surfactant complexes that are fluidlike liquid crystalline at room temperature with hexagonal cylindrical self-assembly. The hexagonal structure with α-helical polypeptide chains is then partially converted to lamellar self-assembly with β-sheet conformation through thermal treatment. We use poly(L-lysine)−dodecylbenzenesulfonic acid complexes, PLL(DBSA)$_x$ ($x = 1.0-3.0$), where the branched dodecyl tails suppress the side-chain crystallization. In the stoichiometric composition, $x = 1.0$, there is one anionic DBSA molecule ionically complexed to each cationic lysine residue. Such a PLL(DBSA)$_{1.0}$ is an infusible solid material at all temperatures until degradation. Introduction of additional DBSA, i.e., $x = 1.5$ or 2.0, plasticizes the material to be shear-deformable and birefringent. In organic solution, as witnessed by small-angle neutron scattering (SANS), the PLL(DBSA)$_x$ complexes form bottle-brush-like cylinders, which upon evaporation of the solvent self-assemble into hexagonal cylindrical morphology with α-helical PLL secondary structure. Heating of PLL(DBSA)$_x$ with $x = 1.0-2.0$ up to the range 120−160 °C leads to the formation of lamellar self-assembled domains with β-sheet conformation of PLL, which coexist with the hexagonal self-assembled structures with α-helical conformation, as shown by Fourier transform infrared spectroscopy (FTIR) and small-angle X-ray scattering (SAXS). Higher complexation ratio, i.e., $x = 3.0$, results in soft and shear-deformable hexagonally packed cylinders at room temperature, but heating irreversibly converts the PLL to a random coil conformation, which leads to a disordered structure. The present model studies show that in polypeptide−surfactant self-assemblies it is possible to change the properties of the material by thermal treatment due to irreversible structural and conformational transformations.

Introduction

Self-assembly, hierarchies, and supramolecular concepts have attracted considerable interest within materials science to achieve new combinations of properties and functions.[1−8] In this perspective, polypeptides can be feasible even beyond their biochemical context,[9] as they can have specific secondary structures and they are biocompatible. The secondary structures can allow a higher level of structural control as well as a possibility for specific functionalities. However, there remain challenges, for example, if polymer-like melt processing methods are required, since the polypeptide-based materials often are infusible. For this purpose, incorporation of spacerlike side chains to polypeptides could be useful. The side chains can be either covalently or alternatively physically bonded, for example by ionic interaction, as will next be discussed.

One of the polypeptides that has gained much interest is poly(L-lysine) (PLL), because it can form both α-helical and β-sheet structures. For example, a smectic A_1 type liquid crystalline packing of β-sheet structures has been achieved by attaching azobenzene side chains covalently to the amine residues of PLL.[10,11] Recently, PLL with side-on linked mesogens has been reported to lead to an α-helical conformation and a thermotropic nematic liquid crystalline behavior.[12] Side-chain substituted PLLs have been shown to form also lyotropic liquid crystals.[13,14] The pitch of the cholesteric mesophase was observed to be tunable by changing the optical purity of the peptide.[13] Covalent modification has also been studied with poly(L-glutamate)s. Poly(α,L-glutamate)s form α-helical structures, which was exploited already in the 80's to prepare thermotropic liquid crystalline materials with covalently substituted alkyl side chains of different lengths.[15−17] The packing of the α-helices was shown to critically depend on the length of the attached alkyl side chains: short chains led to hexagonal packing, whereas long and straight chains, capable of crystallization, induced two-dimensional layered packing of the helices.[16]

More recently, ionic interaction has been used to physically bind amphiphilic side chains to the polypeptide backbone to achieve self-assemblies in the solid state.[18−21] This approach allows facile preparation, but the concept is limited to polypeptides capable of ionic interactions. When aqueous solutions of a polyelectrolyte and an oppositely charged surfactant are combined, a near-stoichiometric complex is precipitated at once from the solution. This method is widely used for synthetic polyelectrolytes, which can form a rich variety of morphologies depending on the structure of the surfactant.[22,23] Also the amount of surfactant used has been found to strongly affect the self-assembly and other properties of polyelectrolyte-based materials, even in conjugated polymers.[24] In the case of polypeptide−surfactant complexes, also the polypeptide backbone secondary structures can affect the self-assembly. Polylysine−surfactant complexes can form both β-sheet and α-helical structures in the solid state, depending on the surfactant and preparation media. The layered structure is favored especially with long *n*-alkylsulfate surfactants.[18,21]

Polypeptide−surfactant complexes studied typically have turned out to be solid mesomorphic, that is, not fluidlike liquid

* Corresponding author. E-mail: Olli.Ikkala@tkk.fi.

10.1021/ma7019495 CCC: $40.75
Published on Web 01/01/2008

crystalline. Thus, there is a need to find a way to plasticize polypeptide-based materials, in order to be able to process them in a facile manner. Additionally, the ultimate materials properties may be required to differ greatly from those needed in processing. This calls for development of new concepts to find self-assembled polypeptide−surfactant complexes, whose properties can be converted after the processing step by an external trigger, most simply by temperature treatment. In the present work, we studied PLL complexed with dodecylbenzenesulfonic acid (DBSA). The stoichiometric complex has been plasticized by additional hydrogen-bonding DBSA, resulting in fluidlike liquid crystallinity. Heat treatment induces irreversible structural and conformational transformations. The materials were studied using SAXS, SANS, FTIR, and polarized optical microscopy.

Experimental Section

Materials. Poly(L-lysine hydrobromide) (PLLHBr, Sigma-Aldrich, 21 500 g mol^{-1}, PDI 1.1 for solid state measurements, and 15 000 g mol^{-1}, PDI 1.1 for solution state measurements), dodecylbenzenesulfonic acid sodium salt (DBSNa, Tokyo Chemical Industry Co., Ltd., soft type), chloroform ($CHCl_3$, Fluka, ≥ 99.8%), silver nitrate ($AgNO_3$, Fluka, ≥ 99.0%), and trifluoroacetic acid (TFA, Fluka, ≥ 98.0%) were used as received. Dodecylbenzenesulfonic acid (DBSA, Tokyo Chemical Industry Co., Ltd., soft type, ≥ 90.0%) was dried in a vacuum. Toluene-d_8 for solution studies was purchased from Aldrich (99.6%) and was used as received.

Complex Preparation. PLLHBr and DBSNa were dissolved in ultrapure Milli-Q water to prepare 1.0 wt % and 0.5 wt % solutions, respectively. When the solutions were combined in a 1:1 molar ratio, a white precipitate was formed immediately. The precipitated solution was further gently mixed for 2 h and filtered with suction (Millipore polypropylene prefilter, 30 μm). The precipitate was rinsed with excess water until the filtrate tested negative for bromide ions. The solid precipitate was vacuum-dried overnight. The resulting complex is denoted as PLL(DBSA)$_{1.0}$ based on the nominal composition, which was also confirmed by elemental analysis. For organic solvent treatment and for further complexation, PLL(DBSA)$_{1.0}$ and DBSA were separately dissolved in $CHCl_3$ containing 3 vol % TFA to prepare 0.5 wt % and 1.0 wt % solutions, respectively. The PLL(DBSA)$_{1.0}$ and DBSA solutions were combined in molar ratios 1:0, 1:0.5, 1:1, and 1:2 to prepare PLL(DBSA)$_x$ with $x = 1.0$, 1.5, 2.0, and 3.0, respectively. After overnight mixing, the solutions were slowly evaporated on Teflon dishes and dried in vacuum at room temperature. For additional solution studies the aforementioned complexes were further dissolved in deuterated toluene-d_8 as 2 wt % solutions with or without 3 vol % of TFA.

Small-Angle X-ray Scattering (SAXS). The solid samples for SAXS measurements were sealed between two Kapton films and measurements were performed with a rotating anode Bruker Microstar microfocus X-ray source (Cu Kα radiation, $\lambda = 1.54$ Å) with Montel Optics. The beam was further collimated with four sets of slits, resulting in a beam area of about 1 mm × 1 mm at the sample position. Scattering intensities were measured using a 2D area detector (Bruker AXS). Sample-to-detector distance was 45 cm. The magnitude of the scattering vector is given by $q = (4\pi/\lambda) \sin \theta$, where 2θ is the scattering angle.

Small-Angle Neutron Scattering (SANS). The behavior of the complexes in solution was probed by small-angle neutron scattering (SANS). Measurements were performed at SANS diffractometer *Yellow Submarine* operating at the Budapest Neutron Centre. Mean neutron wavelength of 5 Å and sample-to-detector distances of 1.3 and 5.6 m provided a useful range of scattering vectors $q = 0.01-0.4$ Å^{-1}. Deuterated toluene-d_8 was used as the solvent in order to increase the contrast between the solvent and the complex. The measurements were performed at 20 °C.

Polarized Optical Microscopy (POM). A Nikon Type 104 polarizing optical microscope with cross polarizers was used with a JVC 3-CCD color video camera to record the images.

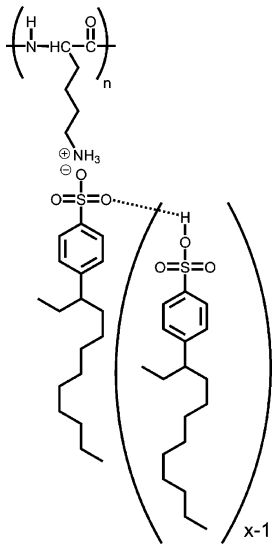

Figure 1. Suggested bonds of PLL(DBSA)$_x$. The stoichiometric complex ($x = 1.0$) forms due to ionic interaction between PLL and DBSA. The binding of additional DBSA in the case of $x > 1.0$ is suggested to be due to hydrogen bonding, where the sulfonic acid groups act as hydrogen-bond donors to the hydrogen-bond accepting sulfonate anions of the ionically bonded DBSA.

Fourier Transform Infrared Spectroscopy (FTIR). For infrared measurements, aqueous precipitated PLL(DBSA)$_{1.0}$ was mixed in a mortar with KBr and pressed to pellets. PLL(DBSA)$_x$ with $x = 1.0$, 1.5, 2.0, and 3.0 were dissolved again in $CHCl_3$ with 3 vol % of TFA, and a few drops were evaporated on silicon wafers and dried in vacuum. Transmission spectra were recorded with Nicolet 380 FTIR spectrometer by averaging 64 spectra with 2 cm^{-1} resolution. The data were further smoothed by EZ Omnic 7.2 Automatic smooth, which uses the Savitsky−Golay algorithm.

Heating. A Linkam TMS 91 temperature controller and a Linkam heating stage were used to control the sample temperature in all the temperature-dependent measurements. The heating rate was 10 °C/min.

Results and Discussion

Room Temperature Behavior in the Solid State. Immediate precipitation took place when the poly(L-lysine hydrobromide) (PLLHBr) and dodecylbenzenesulfonic acid sodium salt (DBSNa) solutions were combined. This is the most direct evidence of the ionic complex formation. Elemental analysis showed a 100% complexation ratio in the limits of experimental error, that is, the complexation took place stoichiometrically. Therefore, we denote the aqueous precipitate by the nominal composition PLL(DBSA)$_{1.0}$ (see Figure 1). After precipitation from aqueous solution and drying, PLL(DBSA)$_{1.0}$ shows absorption peaks in FTIR at 1629 cm^{-1} (amide I), 1694 cm^{-1} (amide I), and 1534 cm^{-1} (amide II), which are characteristic for the β-sheet conformation of the peptide backbone (Figure 2e). SAXS shows a distinct reflection at 0.175 Å^{-1} and a second-order reflection at 0.347 Å^{-1} (Figure 3e), which indicate a well-defined lamellar self-assembly with interlamellar spacing of 36 Å. The precipitated PLL(DBSA)$_{1.0}$ thus consists of alternating layers of PLL β-sheets and surfactant alkyl chains, in accordance with the earlier reported PLL-alkylsulfate complexes prepared from aqueous solution.[18] Such a PLL(DBSA)$_{1.0}$ complex appears hard, brittle and difficult to process due to the β-sheet structure, which does not allow the molecules to flow freely. We expected that if an α-helical secondary structure with hexagonal cylindrical self-assembly was achieved, the chains would gain more mobility. It was previously reported that stoichiometric PLL-alkylsulfate complexes take α-helical conformation when redis-

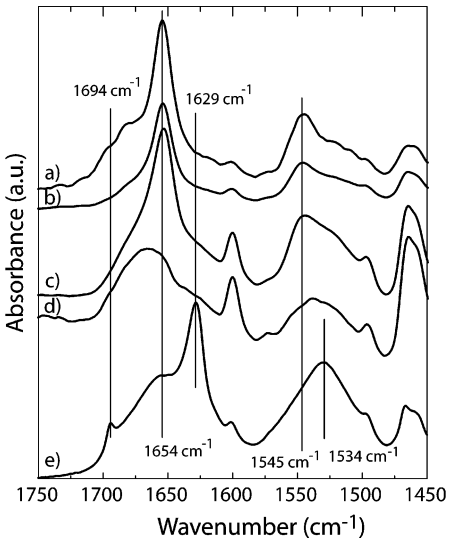

Figure 2. Room-temperature FTIR absorption spectra (a-d) for PLL-$(DBSA)_x$ with $x = 1.0$, 1.5, 2.0, and 3.0, respectively, as prepared from organic solvent. The curve e represents $PLL(DBSA)_{1.0}$ precipitated from aqueous solution.

solved and subsequently dried from organic solvent containing a small amount of trifluoroacetic acid (TFA).[18] However, the structure of the complexes remained lamellar in that case, obviously due to long linear alkyl tails.

In order to study the effect of the organic solvent in the case of surfactants with branched alkyl tails, the aqueous precipitated $PLL(DBSA)_{1.0}$ was dissolved in chloroform containing 3 vol % of TFA to break the hydrogen bonds between the β-sheets. Figure 2a depicts the FTIR spectrum for $PLL(DBSA)_{1.0}$ after drying, which shows a distinct FTIR absorption peak at 1654 cm^{-1} (amide I) and 1545 cm^{-1} (amide II), characteristic of an α-helical structure. Hence, the organic solvent treatment allowed an α-helical secondary structure for $PLL(DBSA)_{1.0}$.The treatment also led to a conversion from lamellar structure to a hexagonal cylindrical self-assembly. This is shown by the SAXS reflections at $q^*_{1.0} = 0.225$ $Å^{-1}$, $2q^*_{1.0}$, $\sqrt{7}q^*_{1.0}$, $3q^*_{1.0}$, $\sqrt{12}q^*_{1.0}$ and $\sqrt{13}q^*_{1.0}$ (inset in Figure 3). The magnitude of $q_{1.0}$* indicates that the intercylinder distance is ca. 32 Å. The hexagonal cylindrical self-assembly of the present $PLL(DBSA)_{1.0}$ complex compared to the previous lamellar self-assembly of polylysine−alkylsulfate complexes[18] is expected to be due to the difference in the alkyl chain packing, as the branched alkyl tails in DBSA cannot pack efficiently enough in order to undergo side-chain crystallization (amorphous alkyl absorption at 2855 and 2927 cm^{-1}, data not shown).

Even if a hexagonal cylindrical self-assembly with α-helical PLL was achieved in organic solvent treated $PLL(DBSA)_{1.0}$, the complex remained solid and hard. Not even heating caused fluidlike softening. By contrast, heating led to a conversion to predominantly lamellar self-assembly with β-sheet PLL conformation, as will be discussed later. Thus, the next aim was to plasticize the hexagonally self-assembled α-helical $PLL(DBSA)_{1.0}$ complex. To achieve this, the hypothesis was that a larger number of plasticizing alkyl side chains must be physically bonded to $PLL(DBSA)_{1.0}$. As the sulfonates are hydrogen-bond acceptors,[25,26] we searched for sufficiently strong hydrogen-bond donors containing alkyl chains to hydrogen bond to the sulfonates of the ionically complexed DBSA. Related work on poly(4-vinylpyridinium methanesulfonate) hydrogen bonded to pentadecylphenol[27] and poly(anilinium camphorsulfonate) hydrogen bonded to alkylresorcinol[28] suggested that $PLL(DBSA)_{1.0}$ could be plasticized with hydrogen-bonded dodecylphenol, pentadecylphenol, or dodecylresorcinol. They turned out, however, to be critical toward macroscopic phase separation, and amphiphilic molecules that are stronger hydrogen-bond donors were searched. In this respect, additional DBSA proved useful. At this point, we want to point out that the strong acidity of DBSA can pose a risk of the polypeptide main chain hydrolysis unless the samples are sufficiently dry. Therefore, the additional hydrogen-bonded DBSA used for plasticization must be regarded only as a model compound. In the current study, all the complexes were carefully dried before measurements, and no signs of hydrolysis were found in any of the measurements. In particular, in FTIR, no absorption peaks of carboxylic acid carbonyls around 1730 cm^{-1} were observed.

The $PLL(DBSA)_{1.0}$ complex and DBSA were dissolved separately in chloroform with 3 vol % of TFA and combined to provide $x = 1.5$, 2.0, and 3.0, followed by slow solvent evaporation and drying. The binding of additional DBSA in the case of $x > 1.0$ could not be directly verified by FTIR due to overlapping bands but is indirectly suggested by the lack of macroscopic phase separation in optical microscopy, composition-dependent softening and changes in the behavior observed in FTIR and SAXS. The birefringence increased with surfactant addition, which is shown in polarized optical micrographs (Figure 4). Indirect further evidence on the binding between DBSA and $PLL(DBSA)_{1.0}$ was gained by SANS measurements on the dissolved complexes (discussed below). The only available hydrogen bond acceptors are the sulfonates[25−28] and the peptide carbonyls. The sulfonates are sterically much less hindered for hydrogen bonding, and we will shortly show arguments suggesting that mainly the sulfonate oxygens actually act as the acceptors.

Whereas the stoichiometric complex appears hard and brittle, $PLL(DBSA)_x$ becomes softer when x is increased, and $PLL(DBSA)_{3.0}$ already behaves as a viscous liquid crystalline fluid. Figures 2 and 3 show the FTIR and SAXS curves for $PLL(DBSA)_x$ at room temperature (curves b−d for $x = 1.5$, 2.0, and 3.0, respectively). A distinct amide I band at 1654 cm^{-1} and amide II band at 1545 cm^{-1} for $PLL(DBSA)_{1.5}$ and $PLL(DBSA)_{2.0}$ show an α-helical secondary structure. In the case of $PLL(DBSA)_{3.0}$, the amide I absorption band is very broad and shifted to a higher wavenumber (1665 cm^{-1}). This indicates that the peptide carbonyl groups undergo much less hydrogen bonding in $PLL(DBSA)_{3.0}$ as compared to $x = 1.0$−2.0. This has two implications. First, the conformation is more disordered due to fewer intramolecular peptide hydrogen bonds. Second, in spite of the large excess of hydrogen bond donors, i.e., DBSA, the carbonyl groups accept only little hydrogen bonding. This further supports the postulation that the additional DBSA molecules make hydrogen bonds to the sulfonates of the ionically complexed DBSA instead of the carbonyl groups.

SAXS (Figure 3) indicates that the chloroform/TFA treated complexes $PLL(DBSA)_x$ have hexagonal cylindrical self-assembly, with the characteristic reflections at $\sqrt{3}q^*_x$ and $2q^*_x$ being more distinct as well as the first-order reflection getting narrower as x is increased from 1.5 to 3.0. Interestingly, the spacing between the cylinders increases only slightly with addition of DBSA: The distance between the helices in $PLL(DBSA)_{3.0}$ is 34 Å as compared to 32 Å in the stoichiometric $PLL(DBSA)_{1.0}$ complex. The small increase in periodicity upon addition of the surfactants can be understood by the 3D helical structure, which indicates that the surfactants are relatively sparsely located at the outer perimeter of the helices. The added hydrogen-bonding surfactants are able to penetrate between the

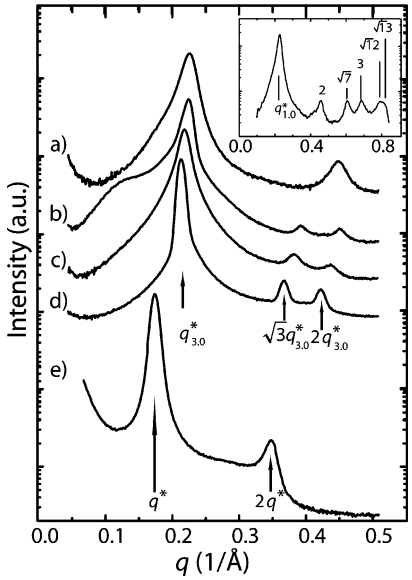

Figure 3. Room-temperature SAXS curves (a-d) for PLL(DBSA)$_x$ with $x = 1.0$, 1.5, 2.0, and 3.0, respectively, as prepared from organic solvent. The inset depicts PLL(DBSA)$_{1.0}$ with larger scattering vector values. Hexagonal cylindrical self-assembly is indicated for a−d. Curve e represents PLL(DBSA)$_{1.0}$ precipitated from water, showing a lamellar self-assembly.

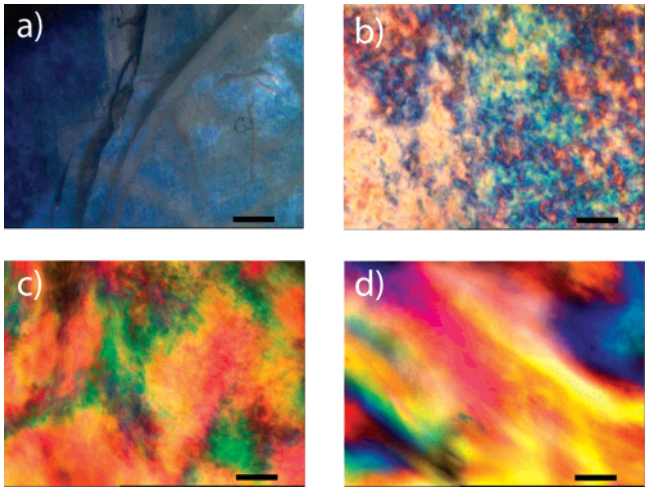

Figure 4. Polarized optical micrographs (a-d) for PLL(DBSA)$_x$ with $x = 1.0$, 1.5, 2.0, or 3.0, respectively, at room temperature as prepared from organic solvent. The scale bar is 50 μm.

ionically attached ones, and therefore, the volume of added surfactants contributes relatively little to the radial dimensions.

Room Temperature Behavior in the Solution State. As the solid-state structure is formed during the solvent evaporation, the behavior of the complexes in the dissolved state can play an important role in the formation of the solid-state structures. In order to study the solution-state behavior using SANS, PLL-(DBSA)$_x$ with $x = 1.0$, 1.5, 2.0, and 3.0 were dissolved in toluene-d_8 in 2 wt % concentration (with or without TFA).

Figure 5 shows scattering data for selected PLL(DBSA)$_x$ complexes in a modified Guinier representation, appropriate for elongated particles. Linearly descending curves are obtained for $q^2 > 0.002$ Å^{-2}, as expected for locally rodlike objects.[29,30] The radius of gyration of the cross section (R_g) can be calculated from the slope of such curves. In the toluene/TFA mixture, the obtained R_g is ca. 12 Å for all cases (see Supporting Information, Table S1), which corresponds to a cylinder radius of 16 Å, assuming that the cylinders are homogeneous. The size agrees

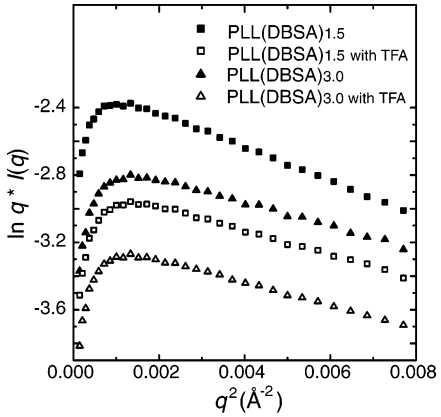

Figure 5. Guinier representation for PLL(DBSA)$_{1.5}$ and PLL(DBSA)$_{3.0}$ dissolved in toluene-d_8 in 2 wt % concentration with and without added TFA (3 vol %).

with the solid-state spacing, as the radii of the cylinders in the solid state are 16−17 Å based on SAXS (Figure 3). This indicates that the cylindrical structure is formed already in solution and not at the moment of solvent evaporation.

SANS data also give information on the stiffness of the helices in the solution, which can be correlated with the ability to form well self-assembled structures in the solid state. The scattering curves were analyzed further within the decoupling approximation,[30,31] according to which the scattering intensity from a sufficiently elongated particle can be written in the form of the product of the scattering function of an infinitely thin chain, $S_{chain}(q)$, and the scattering function of the cross section, $S_{CS}(q)$:

$$I(q) = \text{const} \cdot S_{chain}(q) S_{CS}(q) \quad (1)$$

where

$$S_{CS}(q) = \exp(-q^2 R_g^2/2) \quad (2)$$

The overall shape of the complexes can be characterized by the chain structure factor $S_{chain}(q)$, which is plotted in Figure 6 in a Holtzer plot representation.[31] For all solutions, a plateau region is seen for $q > 0.03$ Å^{-1}, reflecting the overall rigidity of the complexes at an intermediate length scale. For long semiflexible polymers, an upturn of the horizontal data at low q (=q_0)would indicate bending of the polymer, where q_0 gives the persistence length as $l_p \approx 1.9/q_0$.[29] In our case, however, the scattering curves turn down at low q, due to the finite overall size of the complexes. Therefore, the bending of the complexes is not detected from the data and only a lower limit of the persistence length can be calculated as 1.9/0.03 Å^{-1} ≈ 50 Å.

The data appear similar for PLL(DBSA)$_x$ dissolved in pure toluene and toluene/TFA mixture. The only exception, where the horizontal part of the data is clearly shorter, is the PLL-(DBSA)$_{1.0}$, which could be dissolved only with the addition of TFA. The bending of the complexes and their finite size have the opposite effect on the scattering curves. Therefore, the stoichiometric complex seems to be more flexible than the others. Such a behavior indicates that the additional DBSA contributes to the stiffening of the complex ($x > 1.0$) and indirectly shows the interaction of additional DBSA with PLL-(DBSA)$_{1.0}$. This can also be seen in the solid state, where the ordering of the structure improves as the amount of DBSA is increased.

In summary, addition of TFA does not substantially change the shape of the complexes in the solution, and the secondary

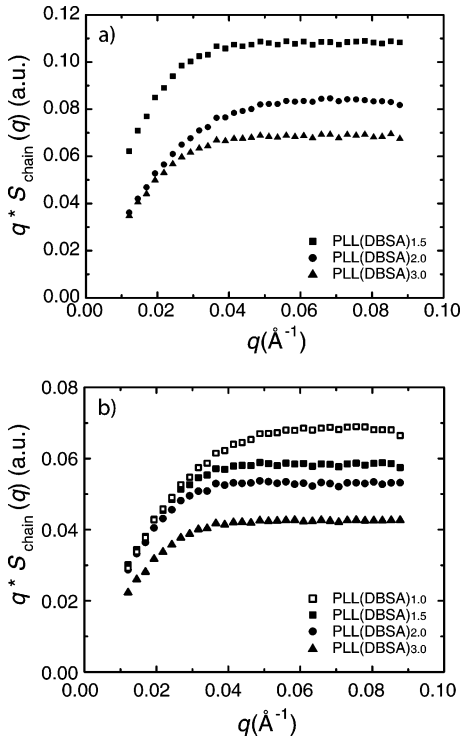

Figure 6. Holtzer plot representation of the chain scattering functions for the complexes in toluene-d_8 in 2 wt % concentration of PLL-(DBSA)$_x$: (a) without and (b) with TFA (3 vol %).

structure of the polymer seems to be unaffected by the acid, at least for $x > 1.0$. This can be argued also to be a sign of the stability of the complexes against hydrolysis. Previous studies on the conformation of PLL−alkylsulfate complexes in chloroform showed that addition of more than 5 vol % of TFA resulted in a change in the secondary structure from α-helix to random coil.[18] We do not observe here any similar effect from the addition of DBSA, probably because DBSA is too bulky to reach the polypeptide backbone. Thus, the DBSA molecules are expected to stay at the outer rim of the complex, and no hydrolysis is envisaged either in the solid state.

Temperature-Dependent Behavior in the Solid State. We above concluded from the room temperature measurements that PLL(DBSA)$_{1.0}$ can exist in two different conformations, leading to two different morphologies: β-sheet conformation with lamellar self-assembly (from water) and α-helical conformation with hexagonal cylindrical self-assembly (from $CHCl_3$/TFA). Since the β-sheet conformation is often observed for PLL at elevated temperatures,[19,32−34] we next studied the effect of heating on the structures of the chloroform treated PLL(DBSA)$_x$ complexes in the solid state. A transition from α-helix to β-sheet conformation was expected. Related α-helix to β-sheet transition has been reported earlier for *Bombyx mori* cocoon silk fiber, which showed an α-helical structure when prepared from hexafluoro-2-propanol and which turned to β-sheet at 140 °C.[35]

After casting from organic solvent, PLL(DBSA)$_x$ with $x =$ 1.0, 1.5, and 2.0 show at room temperature in FTIR an amide I absorption at 1654 cm^{-1} (Figure 7a-c), indicating an α-helical secondary structure as discussed above. Upon heating to 140−160 °C, a new amide I band arises at 1625 cm^{-1}, while the initial band at 1654 cm^{-1} becomes drastically reduced. This indicates that the structures undergo a partial conformational change from α-helix to β-sheet. At ca. 160 °C also a weaker absorption at 1692 cm^{-1} is formed, supporting an antiparallel conformation. The resulting antiparallel β-sheet conformation has been suggested to derive from the pre-transitional, energetically favored antiparallel alignment of the dipolar α-helices.[33,34] Similar antiparallel orientation of α-helices was also previously reported by us in the context of self-assembling diblock copolypeptide−surfactant complexes.[36] For $x = 3.0$, on the other hand, at room temperature a broad peak at 1667 cm^{-1} is observed, suggesting a less ordered α-helical conformation (see discussion above). Curiously, when the sample is heated up to 120 °C, a clear narrowing of the peak is observed with a concurrent shift to a lower wavenumber, 1654 cm^{-1} (Figure 7d). This suggests improving α-helicity upon heating. However, further heating to 140 °C induces a broadening and a shift of the amide I band to higher wavenumbers, which indicates reduced hydrogen bonding and more conformational disorder. The transitions observed by FTIR are irreversible, i.e., the structures remain after cooling to room temperature.

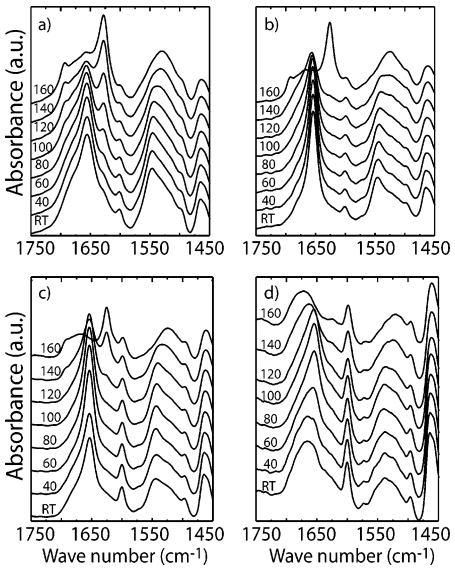

Figure 7. FTIR spectra for PLL(DBSA)$_x$ as a function of temperature: (a) $x = 1.0$, (b) $x = 1.5$, (c) $x = 2.0$, and (d) $x = 3.0$.

Also SAXS shows different temperature behavior for PLL-(DBSA)$_{3.0}$ compared to the other complexes (Figure 8). Distinct reflections at $q^*_{3.0} = 0.22$ Å^{-1}, $\sqrt{3}q^*_{3.0}$ and $2q^*_{3.0}$ indicate a cylindrical hexagonal structure at room temperature (Figure 8d), but as the complex is heated past ca. 120 °C, the main reflection starts to broaden, and as the temperature reaches ca. 140 °C, the higher order reflections disappear and do not reappear during cooling. This means that an irreversible loss of structure takes place, coinciding with the loss of secondary structure observed in FTIR and the loss of birefringence in POM (see Supporting Information). In other words, the PLL(DBSA)$_{3.0}$ complex undergoes an irreversible transition to disordered state between 120 and 140 °C. For the complexes with $x = 1.0$, 1.5, and 2.0, on the other hand, the hexagonal cylindrical self-assembly adopted at room temperature is observed to persist even upon heating, although the intensity is slightly reduced (Figure 8a−c). But interestingly, a new reflection appears at $q^{**}_x =$ 0.184−0.189 Å^{-1} as the temperature passes ca. 100 °C. For the stoichiometric complex, $x = 1.0$, the new reflection is accompanied by a faint second-order reflection at $2q^{**}_{1.0}$ at 160 °C, indicating a coexistent lamellar structure. Even if the second-order reflections cannot be resolved for $x = 1.5$ and 2.0, we expect that also in those cases the structure corresponding to $q^{**}_x = 0.184-0.189$ Å^{-1} is lamellar. The lamellar periodicity corresponds well to the distance between the cylinders at room temperature, i.e., 32−34 Å. Additionally, the polarized optical micrographs show birefringence for PLL(DBSA)$_x$ with $x = 1.0$,

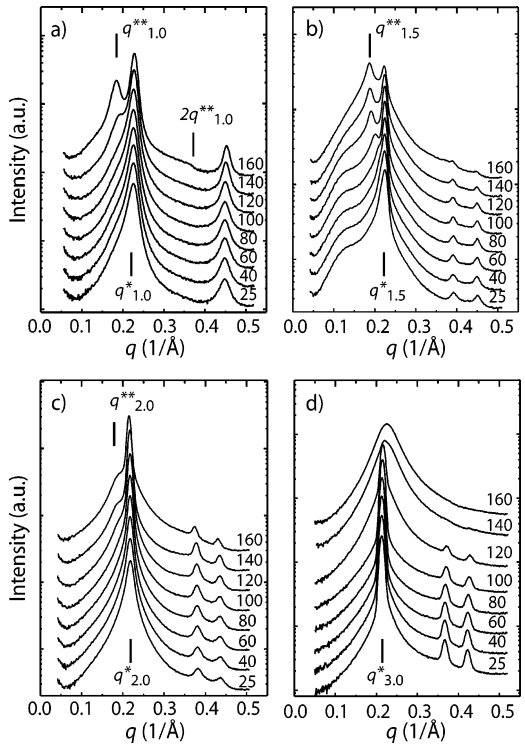

Figure 8. SAXS graphs of the PLL(DBSA)$_x$ complexes as a function of temperature: (a) $x = 1.0$, (b) $x = 1.5$, (c) $x = 2.0$, and (d) $x = 3.0$. Curves similar to the ones at 160 °C remain after cooling.

1.5, and 2.0 at all studied temperatures (see Supporting Information), in agreement with the mesomorphic structures observed in SAXS. Finally, we want to point out that different characterization techniques required different methods for sample preparation, which might have led to the small differences between the transition temperatures in FTIR and SAXS.

To summarize, in organic solvent, PLL(DBSA)$_x$ with $x = 1.0-3.0$ consist of highly elongated bottle-brush-like objects based on SANS (Figure 5), schematically shown in Figure 9. PLL(DBSA)$_x$ complexes cast from organic solvent appear at room temperature in an α-helical secondary structure (Figure 2) and hexagonal cylindrical self-assembly (Figure 3), which is also schematically illustrated in Figure 9. The complex PLL(DBSA)$_{1.0}$ is hard and infusible but added DBSA induces plasticization, enabling shear deformation. For $x = 1.0-2.0$, FTIR shows that heating to 120−160 °C leads to a partial transformation to β-sheet conformation while some α-helicity is simultaneously preserved (Figure 7a−c). Similarly, SAXS shows that new reflections emerge upon heating. These reflections are attributed to the formation of a coexistent lamellar structure, while the hexagonal cylindrical self-assembly is still partly retained (Figure 8a−c). This means that for $x = 1.0-2.0$, β-sheet secondary structures tend to be formed in the melt/solid state upon heating, but this transformation cannot run into completeness, and a mixed state consisting of both hexagonal cylindrical self-assembly with α-helical conformation and lamellar self-assembly with β-sheet conformation is obtained. If the β-sheet structures start growing in several locations at the same time upon heating, the α-helices can be trapped between the different β-sheet domains, which could explain the observed mixed phase. We also emphasize that in order to have well-defined self-assemblies, annealing is usually required, which could not be properly done in the present system.

PLL(DBSA)$_{3.0}$ forms cylindrical hexagonal self-assembly with a less-ordered α-helical secondary structure at room temperature. The material is soft and shows birefringence in optical microscopy. Upon heating, the order is lost between 120 and 140 °C (Figures 7d and 8d), in agreement with the loss of birefringence. At 160 °C, PLL(DBSA)$_{3.0}$ appears as a readily flowing fluid. This is interpreted as an irreversible transition from a self-assembled structure to a disordered structure. The different behavior of the PLL(DBSA)$_{3.0}$ is reasonable, since in that complex PLL contributes only to 11.6 wt % in the material. At this high dilution of PLL in DBSA, β-sheets are no longer able to form and the chains adopt a random coil conformation after heating.

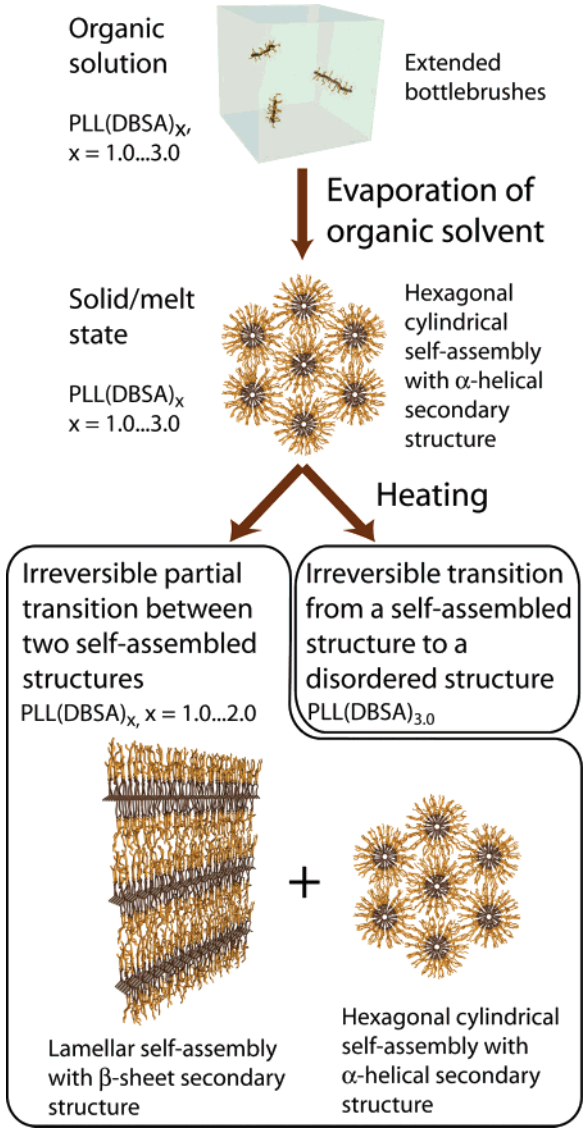

Figure 9. Scheme for the structure evolution of PLL(DBSA)$_x$. Extended bottle-brush-like objects are formed in organic solvent for $x = 1.0-3.0$. In solid/melt state, all the complexes form hexagonal cylindrical self-assembly with α-helical secondary structure at room temperature showing increasing softening with higher x. Upon heating, a mixed phase is observed for $x = 1.0$, 1.5, and 2.0 containing also domains of lamellar self-assembly with β-sheet secondary structure. The highly plasticized complex PLL(DBSA)$_{3.0}$, however, becomes disordered upon heating.

Conclusions

We introduced plasticization of self-assembled polypeptide−surfactant complexes in the melt/solid state to achieve fluidlike liquid crystallinity. The irreversible conformational transitions of the peptide secondary structures and their effect on the self-assembly were shown as a function of temperature. Poly(L-lysine

hydrobromide) (PLLHBr) was stoichiometrically complexed by ionic interaction with dodecylbenzenesulfonic acid sodium salt (DBSNa), which has a branched dodecyl tail. The complex is denoted as PLL(DBSA)$_{1.0}$ based on its nominal composition. The rigid and solid PLL(DBSA)$_{1.0}$ was plasticized with hydrogen-bonded additional dodecylbenzenesulfonic acid (PLL(DBSA)$_x$). In organic solution, the complexes were shown to act as bottle-brush-like cylinders, the structure of which was maintained and even stabilized by the addition of more than stoichiometric amount of the surfactant. In the solid state the softness and fluidlike character were found to improve, as the amount of additional DBSA was increased. With $x = 1.5$ and 2.0, a fluidlike liquid crystalline material with an α-helical secondary structure of PLL and hexagonal cylindrical self-assembly was achieved. Heating past 120−140 °C led to a partial change to lamellar self-assembly with a β-sheet secondary structure. The heating thus produced a mixed structure, where the complete conversion was inhibited probably due to topological constraints. For $x = 3.0$, the heating brought disordered structure with a random coil conformation. All transitions were irreversible in the time scale of the measurements.

We anticipate that the shown schemes open new routes to develop polypeptide materials, whose properties before and after processing could be tuned separately. The fluidlike properties based on hexagonal cylindrical self-assembly of α-helical polypeptides could be converted to interlocking lamellar β-sheet structure by an external trigger. Here, the liquid crystalline processing of silk and the insoluble final product, which is achieved by a pH change and elongation, is of course the great, albeit very complex and distant model. Our present study suggests pursuing related simpler systems, but considerable insight and work are required in selecting the starting materials, their bonding and functionalities.

Acknowledgment. We want to thank Panu Hiekkataipale for his assistance in the SAXS experiments and visiting professor Charl Faul for discussions. The neutron scattering experiments have been supported by the European Commission under the Sixth Framework Program through the Key Action, Strengthening the European Research Area, Research Infrastructures, Contract No. RII3-CT-2003-505925. The Academy of Finland and its Center of Excellence ("Bio- and Nanopolymers Research Group", 77317), as well as the Jenny and Antti Wihuri Foundation and the Marie Curie Network PolyAmphi, are thanked for financial support.

Supporting Information Available: Additional experimental details can be found in supporting information, including a table of gyration radii for the complexes in solution, figures of TGA experiments, a TEM micrograph, and polarized optical micrographs of temperature treated samples. This material is available free of charge via the Internet at http://pubs.acs.org.

References and Notes

(1) Whitesides, G. M.; Mathias, J. P.; Seto, C. T. *Science* **1991**, *254*, 1312−1319.
(2) Muthukumar, M.; Ober, C. K.; Thomas, E. L. *Science* **1997**, *277*, 1225−1232.
(3) Percec, V.; Ahn, C.-H.; Ungar, G.; Yeardley, D. J. P.; Möller, M.; Sheiko, S. S. *Nature (London)* **1998**, *391*, 161−164.
(4) Faul, C. F. J.; Antonietti, M. *Adv. Mater.* **2003**, *15*, 673−683.
(5) Ikkala, O.; ten Brinke, G. *Chem. Commun.* **2004**, 2131−2137.
(6) Hoeben, F. J. M.; Jonkheijm, P.; Meijer, E. W.; Schenning, A. P. H. J. *Chem. Rev.* **2005**, *105*, 1491−1546.
(7) Kato, T.; Mizoshita, N.; Kishimoto, K. *Angew. Chem., Int. Ed. Engl.* **2006**, *45*, 38−68.
(8) ten Brinke, G.; Ruokolainen, J.; Ikkala, O. *Adv. Polym. Sci.* **2007**, *207*, 113−177.
(9) McGrath, K.; Kaplan, D., Eds. *Protein-Based Materials*; Birkhäuser: Boston, MA, 1996.
(10) Gallot, B.; Fafiotte, M.; Fissi, A.; Pieroni, O. *Macromol. Rapid Commun.* **1996**, *17*, 493−501.
(11) Gallot, B.; Fafiotte, M.; Fissi, A.; Pieroni, O. *Liq. Cryst.* **1997**, *23*, 137−146.
(12) Schaefer, K. E.; Keller, P.; Deming, T. J. *Macromolecules* **2006**, *39*, 19−22.
(13) Bellomo, E. G.; Davidson, P.; Impéror-Clerc, M.; Deming, T. J. *J. Am. Chem. Soc.* **2004**, *126*, 9101−9105.
(14) Yu, M.; Nowak, A. P.; Deming, T. J. *J. Am. Chem. Soc.* **1999**, *121*, 12210−12211.
(15) Watanabe, J.; Fukuda, Y.; Gehani, R.; Uematsu, I. *Macromolecules* **1984**, *17*, 1004−1009.
(16) Watanabe, J.; Ono, H.; Uematsu, I.; Abe, A. *Macromolecules* **1985**, *18*, 2141−2148.
(17) Daly, W. H.; Poché, D.; Negulescu, I. I. *Prog. Polym. Sci.* **1994**, *19*, 79−135.
(18) Ponomarenko, E. A.; Tirrell, D. A.; MacKnight, W. J. *Macromolecules* **1996**, *29*, 8751−8758.
(19) Ponomarenko, E. A.; Tirrel, D. A.; MacKnight, W. J. *Macromolecules* **1998**, *31*, 1584−1589.
(20) MacKnight, W. J.; Ponomarenko, E. A.; Tirrell, D. A. *Acc. Chem. Res.* **1998**, *31*, 781−788.
(21) Wenzel, A.; Antonietti, M. *Adv. Mater.* **1997**, *9*, 487−490.
(22) Antonietti, M.; Conrad, J.; Thünemann, A. *Macromolecules* **1994**, *27*, 6007−6011.
(23) Antonietti, M.; Burger, C.; Thünemann, A. *Trends Polym. Sci.* **1997**, *5*, 262−267.
(24) Zheng, W.-Y.; Wang, R.-H.; Levon, K.; Rong, Z. Y.; Taka, T.; Pan, W. *Macromol. Chem. Phys.* **1995**, *196*, 2443−2462.
(25) Russell, V. A.; Evans, C. C.; Li, W.; Ward, M. D. *Science* **1997**, *276*, 575−579.
(26) Russell, V. A.; Ward, M. D. *Chem. Mater.* **1996**, *8*, 1654−1666.
(27) Ruokolainen, J.; Mäkinen, R.; Torkkeli, M.; Mäkelä, T.; Serimaa, R.; ten Brinke, G.; Ikkala, O. *Science* **1998**, *280*, 557−560.
(28) Kosonen, H.; Ruokolainen, J.; Knaapila, M.; Torkkeli, M.; Jokela, K.; Serimaa, R.; ten Brinke, G.; Bras, W.; Monkman, A. P.; Ikkala, O. *Macromolecules* **2000**, *33*, 8671−8675.
(29) Menge, U.; Lang, P.; Findenegg, G. H.; Strunz, P. *J. Phys. Chem. B* **2003**, *107*, 1316−1320.
(30) Muroga, Y.; Yoshida, T.; Kawaguchi, S. *Biophys. Chem.* **1999**, *81*, 45−57.
(31) Pedersen, J. S.; Egelhaaf, S. U.; Schurtenberger, P. *J. Phys. Chem.* **1995**, *99*, 1299−1305.
(32) Davidson, B.; Fasman, G. D. *Biochemistry* **1967**, *6*, 1616−1629.
(33) Dzwolak, W.; Muraki, T.; Kato, M.; Taniguchi, Y. *Biopolymers* **2004**, *73*, 463−469.
(34) Dzwolak, W.; Smirnovas, V. *Biophys. Chem.* **2005**, *115*, 49−54.
(35) Drummy, L. F.; Phillips, D. M.; Stone, M. O.; Farmer, B. L.; Naik, R. R. *Biomacromolecules* **2005**, *6*, 3328−3333.
(36) Hanski, S.; Houbenov, N.; Ruokolainen, J.; Chondronicola, D.; Iatrou, H.; Hadjichristidis, N.; Ikkala, O. *Biomacromolecules* **2006**, *7*, 3379−3384.

MA7019495